Dynamics of cD Clusters of Galaxies. IV. Conclusion of a Survey of 25 Abell Clusters

William R. Oegerle^{1,2}, John M. Hill³

ABSTRACT

We present the final results of a spectroscopic study of a sample of cD galaxy clusters. The goal of this program has been to study the dynamics of the clusters, with emphasis on determining the nature and frequency of cD galaxies with peculiar velocities. Redshifts measured with the MX Spectrometer have been combined with those obtained from the literature to obtain typically 50 - 150observed velocities in each of 25 galaxy clusters containing a central cD galaxy. We present a dynamical analysis of the final 11 clusters to be observed in this sample. All 25 clusters are analyzed in a uniform manner to test for the presence of substructure, and to determine peculiar velocities and their statistical significance for the central cD galaxy. These peculiar velocities were used to determine whether or not the central cD galaxy is at rest in the cluster potential well. We find that 30 - 50% of the clusters in our sample possess significant subclustering (depending on the cluster radius used in the analysis), which is in agreement with other studies of non-cD clusters. Hence, the dynamical state of cD clusters is not different than other present-day clusters. After careful study, four of the clusters appear to have a cD galaxy with a significant peculiar velocity. Dressler-Shectman tests indicate that three of these four clusters have statistically significant substructure within $1.5h_{75}^{-1}~{
m Mpc}$ of the cluster center. The dispersion of the cD peculiar velocities is 164^{+41}_{-34} km s⁻¹ around the mean cluster velocity. This represents a significant detection of peculiar cD velocities, but at a level which is far below the mean velocity dispersion for this sample of clusters. The picture that emerges is one in which cD galaxies are nearly at rest with respect to the cluster potential well, but have small residual velocities due to subcluster mergers.

¹Department of Physics & Astronomy, Johns Hopkins University, Baltimore, MD 21218-2695

²current address: Laboratory for Astronomy and Solar Physics, Code 681, Goddard Space Flight Center, Greenbelt, MD 20771. Email: william.oegerle@gsfc.nasa.gov

³Steward Observatory, University of Arizona, Tucson, AZ 85721-0065. Email: jhill@as.arizona.edu

Subject headings: galaxies: clusters: general — galaxies: clusters: Individual (A779, A1691, A1749, A1767, A1837, A1927, A2061, A2067, A2079, A2089, A2199, A2666) — galaxies: cD — galaxies: redshifts — galaxies: kinematics and dynamics

1. INTRODUCTION

First-ranked elliptical galaxies in clusters, also referred to as brightest cluster galaxies (BCGs), are the brightest and most massive galaxies in the universe. About 20% of BCGs are surrounded by large, low surface brightness envelopes, and are called cD galaxies. cDs exist only in clusters and groups and never in the field. Their existence and evolution are intimately tied to the formation and evolution of the clusters themselves. Although a wealth of data on the properties of cD galaxies exists, it is still unknown whether cDs are the products of dynamical processes operating in clusters prior to their collapse or after cluster virialization.

Clues to the formation of cD galaxies may be found in kinematic studies of cDs and their parent clusters. The properties of cD galaxies are generally consistent with the galaxy lying at the bottom of the cluster potential well. They are located at clusters centers (Matthews, Morgan, & Schmidt 1964), and they are located at the peak of the cluster X-ray emission (Jones et al. 1979). Quintana & Lawrie (1982) investigated the kinematics of nine cD clusters and concluded that all the cD galaxies in their sample were at rest with respect to their parent clusters within the observational uncertainties. More recent work with better determination of velocity distributions has revealed several cases where a cD galaxy has a statistically significant peculiar velocity with respect to its parent cluster (Sharples, Ellis & Gray 1988; Hill et al. 1988; Oegerle & Hill 1994).

In the "cannibalism" model of cD formation, large galaxies at the center of a cluster merge to form a cD which then continues to grow through accretion of cluster galaxies (Hausman & Ostriker 1978). If these mergers happened long ago, then dynamical friction should have settled the cD galaxy to rest at the bottom of the cluster potential well. However, strong cannibalization seems to have been ruled out by the observational studies of Lauer (1988) who concludes that this mechanism cannot solely account for the large luminosity ($\sim 10L^*$) of cD galaxies. Merritt (1985) argued that the tidal field in clusters will disrupt galaxy halos, thereby lengthening the dynamical friction timescale and acting to diminish cannibalism. Merritt proposed that cDs are formed early in life of a cluster, and that the cD must form at the dynamical center of the cluster to avoid tidal truncation of its envelope. Dubinski (1998) has simulated the formation of a cluster in a hierarchical cosmological model,

and shown that a BCG will form early in the cluster's history at the cluster center through the mergers of several massive galaxies flowing inward along filaments. The photometric and internal kinematic properties of the simulated BCG bear a striking resemblance to the observed properties of real BCGs, although the simulation did not produce the extended low-surface brightness envelopes associated with cD galaxies. This simulation was carried out with initial conditions that led to a fairly poor cluster at the present epoch (59 galaxies), and did not include the possible effects of subcluster mergers that one might expect in the hierarchical formation of a rich cluster.

If clusters are formed through the hierarchical merging of smaller clusters, then cDs would be formed in one of these merging subclusters. We could then hope to detect the residual motion of the cD with respect to the merging clusters. Malumuth (1992) has explored with simulations whether it is possible to form cD galaxies with significant peculiar velocities in rich clusters via dynamical friction. He found that after $\sim 10^{10}$ years, the cD galaxies in his simulated clusters had a distribution of peculiar velocities which was significantly different than the observed clusters. The efficiency of dynamical friction and 2-body relaxation over that timescale resulted in the cD being dragged to the bottom of the potential well with little peculiar velocity. He concluded that his models could be reconciled with observations only if: 1) clusters which form cD galaxies are relatively young; 2) cD galaxies are a relatively recent phenomenon; 3) clusters are not entirely virialized; 4) cD galaxies are not formed in their present environment, but have been added from elsewhere; or 5) dynamical friction in the real universe is not as efficient as in the simulations.

The observational data employed by Malumuth (1992) for comparison with his models were culled from many different sources in the literature, which used different data reduction and analysis techniques, and was not an objective sample of clusters. Having established that at least some cD galaxies have significant peculiar velocities, Hill & Oegerle (1993) began a systematic survey to determine the accurate peculiar velocities of cD galaxies in a statistically complete sample of clusters. This survey also included extensive dynamical study of the host clusters. The object of the survey was to determine if the known peculiar velocities of cDs represent the statistical tail of a distribution of velocities where the cD galaxy is at rest in the cluster potential, or whether the peculiar velocities were telling us something important about the process of cD and cluster formation. This paper represents the conclusion of that systematic survey.

The questions that we attempt to answer here are whether cD galaxies in rich clusters have significant peculiar velocities relative to the cluster potential well, and whether the number and distribution of those peculiar velocities are able to constrain the models of cD formation and growth.

In section 2 we review the selection and subsequent expansion of the cluster sample for this study. In section 3 we provide a detailed dynamical analysis of the 11 clusters which were observed by Hill & Oegerle (1998). In section 4 we discuss the observed cD peculiar velocities and the effects of substructure in the clusters. In section 5, we briefly review the formation scenarios for cD galaxies. Finally in section 6 we report the conclusions of this study.

2. CLUSTER SAMPLE

In order to arrive at a tractable sample of clusters, we started in with the Hoessel et al. (1980) (HGT) Abell cluster sample (Hill & Oegerle 1993) (Paper I). HGT selected their sample of brightest cluster galaxies from all northern Abell clusters with: (a) absolute values of galactic latitude larger than 30°, (b) richness class ≥ 1 and distance class ≤ 4 , and (c) richness class 0 and distance class ≤ 3 . We have further narrowed the HGT sample using the following additional constraints: (1) the cluster must be of Rood-Sastry type cD as defined by Struble & Rood (1987), (2) have redshift < 0.08, and (3) have declination $-11^{\circ} < \delta < +72^{\circ}$. All of our observations were obtained on Kitt Peak in Arizona, hence the lower declination cut-off at -11° . The upper declination cut-off of $+72^{\circ}$ was due to a telescope limit when observing with the MX multifiber spectrometer.

During the course of this study we discovered that cluster A1927 actually had a mean redshift of 0.0948 placing it outside our original sample constraints. In order to retain A1927 in our sample and keep the sample complete, we have expanded the redshift limit to 0.095 and included A1651 in the sample. The resulting sample of 25 Abell clusters is listed in Table 1.

Datasets of suitable size and quality for use in this study now exist in the literature for some of the clusters in our sample. Redshifts for A2670 have been published by Sharples, Ellis & Gray (1988). Redshift data for A85 and A2052 have been published by Malumuth et al. (1992). As a part of our program, we have previously published data for A2107 (Oegerle & Hill 1992), and A2634 (Pinkney et al. 1993). In Paper I, we presented redshifts for A193, A399, A401, A1795, A1809, A2063, and A2124. Redshifts for A2029 were presented by Oegerle, Hill & Fitchett (1995) as part of another study. In Hill & Oegerle (1998) (Paper III) we presented redshift data for A779, A1691, A1749, A1767, A1837, A1927, A2067, A2079, A2089, A2199 and A2666.

Throughout this paper we have used $q_o = 1/2$, and parameterized the Hubble constant by using the term h_{75} , where $H_o = 75h_{75}$ km s⁻¹ Mpc⁻¹.

3. KINEMATICS OF THE 11 NEWLY OBSERVED CLUSTERS

In this section, we present an analysis of the 11 galaxy clusters for which redshift data was published in Hill & Oegerle (1998), complementing previous analyses of the other clusters in our sample published previously (and cited above.) First we discuss the velocity distributions and dispersions of these clusters, and then investigate evidence for substructure. This is followed by notes on individual clusters which warrant further discussion.

3.1. Velocity Distributions

We have supplemented our observations with additional velocities from the literature within a radius of approximately $3.5h_{75}^{-1}$ Mpc. In general we have tried to be complete through mid-1998 when adding velocities from the literature. It should be noted, however, that not all clusters have redshift data out to a radius as large as $3.5h_{75}^{-1}$ Mpc.

To determine cluster membership, we have employed the " 3σ clipping" technique of Yahil & Vidal (1977), with a slight variation. All computations are made not on the observed heliocentric-corrected velocities but on their cosmologically corrected values: v = $c[(1+z)^2-1]/[(1+z)^2)+1]$. Initially, we exclude from the distribution any galaxy more than 6000 km s⁻¹ from the velocity of the brightest cluster galaxy (BCG). We chose to cut around the velocity of the BCG rather than the median velocity of all galaxies in the sample in order to minimize the effects of background groups and clusters and the surrounding supercluster environment. After making this cut, we then proceed with the 3σ clipping as described by Yahil & Vidal (1977). The mean velocity and dispersion are computed from the remaining galaxies, and then the galaxy furthest from the mean is clipped from the distribution if it is more than 3σ distant. The mean and dispersion are recomputed after each galaxy is clipped. This procedure is followed until the furthest outlying galaxy is accepted as a cluster member, at which point the clipping procedure is halted. Determination of membership is usually straightforward for most clusters in our sample, with several notable exceptions that are discussed below. In addition to computing the mean and standard deviation (dispersion) of the cluster members, we have also computed the more robust quantities, C_{bi} and S_{bi} , which are biweight measures of location and scale as described by Beers, Flynn & Gebhardt (1990). When computing these values, the 3σ clipping technique is not used at all. Instead, these robust quantities are computed from all galaxy velocities within $\pm 6000~{\rm km\,s^{-1}}$ of the velocity of the BCG.

The histograms of observed velocities for the 11 clusters are shown in Figure 1. In the figures, the arrow marks the observed velocity of the cD galaxy and the dashed line is a

normalized Gaussian, centered at C_{bi} , with a dispersion equal to $\sigma = (1+z)S_{bi}$ computed from all galaxies within $3.5h_{75}^{-1}$ Mpc. The Gaussian extends to $\pm 3\sigma$ in velocity. All galaxy velocities within ± 6000 kms⁻¹ from C_{bi} are plotted in Figure 1, not just the cluster members.

The mean observed cluster velocities (heliocentric cz in km s⁻¹), velocity dispersions corrected for measurement error, and values of biweight location, C_{bi} , and scale, S_{bi} , are given in Table 1 for these 11 clusters plus the other 14 clusters in the sample. The velocity data for all of the clusters have been reanalyzed according to the cluster membership criteria discussed above. Thus the results in Table 1 may differ from those previously reported in the literature because of small algorithmic differences or because of additional redshifts which have been measured since the original analysis. The first line for each cluster listed in Table 1 is computed for all known redshifts within $3.5h_{75}^{-1}$ Mpc of the BCG. Since not all clusters have measured redshifts extending out as far as $3.5h_{75}^{-1}$ Mpc, we have added a second line in Table 1 computed for all known redshifts within $1.5h_{75}^{-1}$ Mpc. In cases where the cluster is part of a larger supercluster environment, or if subclustering exists at large radii, the result based on galaxies within $1.5h_{75}^{-1}$ Mpc possibly provides a more meaningful picture of the true dynamical state of the cluster, at least with respect to any peculiar velocity of the cD.

3.2. Substructure

To investigate the shape of the cluster velocity distributions, we have calculated the I statistic, which is a sensitive indicator of non-Gaussian distributions (Teague, Carter & Gray 1990). A distribution is considered non-Gaussian if $I > I_{0.90}$, where $I_{0.90}$ is the critical value for rejecting the Gaussian hypothesis at the 90% confidence level. The values of I and $I_{0.90}$ are given in Table 2, where we have once again presented results for two cutoffs in the outer radius of the cluster. With an outer radius of $1.5h_{75}^{-1}$ Mpc, all clusters pass the Gaussian test except A1749 and A1927. A1749 has a tail to the velocity distribution extending to larger velocities. A1927 is interesting in that the distribution of galaxies within $3.5h_{75}^{-1}$ Mpc is Gaussian, but not if the radius is restricted to 1.5 Mpc. This will be discussed further below. A2079 and A2089 appear non-Gaussian when including galaxies from a larger radius, but this is due to their location within the Corona Borealis supercluster. Cluster velocity dispersions do change as a function of cluster radius as illustrated by the detailed analysis of A2063 by Krempeć-Krygier & Krygier (1999).

We have employed the Dressler-Shectman Δ test (Dressler & Shectman 1988) as an additional means of searching for the presence of substructure in velocity and/or dispersion. For each cluster member, the term $\delta_n^2 = 11[(\bar{v}_{local} - \bar{v}_{cl})^2 + (\sigma_{local} - \sigma_{cl})^2]/\sigma_{cl}^2$ is calculated, where \bar{v}_{local} and σ_{local} are the mean velocity and dispersion for the 10 nearest neighbor galax-

ies, and \bar{v}_{cl} and σ_{cl} are the global cluster values. For each cluster, we have plotted circles at the position of each galaxy in Figure 3, where the diameter of the circle is proportional to e^{δ} . A large circle (i.e. large value of δ) indicates a galaxy which is deviant in either velocity or dispersion compared to nearby galaxies (projected on the sky). A single large circle does not indicate anything statistically significant, but groups of large circles do indicate the presence of subclustering in velocity or dispersion. The cumulative deviation of a cluster, Δ_{obs} , is then computed by summing δ_n over all n observed galaxies. The statistical significance of the deviation is determined by Monte Carlo simulations in which the observed velocities are randomly assigned to galaxies at the observed galaxy locations, and Δ_{sim} is computed for each of these simulated clusters. For each of the 11 clusters under study here, we have constructed 1000 simulated clusters and computed Δ_{sim} for each simulation. The results are shown in Table 2, where we list Δ_{obs} and the fraction of simulated clusters with $\Delta_{sim} > \Delta_{obs}$. Clusters with very small values of $f(\Delta_{sim} > \Delta_{obs})$ contain statistically significant subclustering. For example, from Table 2, A2670 has $f(\Delta_{sim} > \Delta_{obs}) = 0.002 - 0.004$ depending on the radius of included galaxies - only 2-4 simulated clusters out of 1000 simulations had $\Delta_{sim} > \Delta_{obs}$. This indicates subclustering which is significant at the $\gtrsim 3\sigma$ level.

3.3. A779

A779 presents a real difficulty for the 3σ clipping technique, since there are galaxies spread over a large range of velocities. A779 is at low redshift ($z \sim 0.023$) and therefore, its projected size on the sky is quite large when considering as potential members all galaxies within a radius of $3.5h_{75}^{-1}$ Mpc. The initial dispersion computed from the distribution is so large that effectively no galaxies are clipped (beyond the initial $\pm 6000~\rm km s^{-1}~cut$). Hence, the standard velocity dispersion computed for this distribution is extremely large – $2256~{\rm km\,s^{-1}}$ as reported in Table 1. The 3σ clipping technique arrives at different results depending the somewhat arbitrary decision to limit the initial cluster galaxy sample to those galaxies within ± 6000 km s⁻¹. If the cut were decreased to only ± 5000 km s⁻¹, then the procedure successfully eliminates velocity outliers and arrives at a dispersion of $\sigma = 489~{\rm km}~{\rm s}^{-1}!$ The more robust biweight scale, S_{bi} is 741 km s⁻¹. The Gaussian overlay in Figure 1 is drawn using this value of S_{bi} , but still appears somewhat broader than the true velocity distribution. The value of S_{bi} computed within a radius of $1.5h_{75}^{-1}$ Mpc is about 30% smaller (512 km s⁻¹ as reported in Table 1), and appears to be a better representation of the dispersion of the true cluster. A quick look at Fig 3a indicates why the computed dispersion is so large when galaxies at large radii are included. There are a number of galaxies ~ 5000 arcsec to the NE of A779 which lie far from the central velocity of the cluster. A cutoff radius of $1.5h_{75}^{-1}~{\rm Mpc}$ at this redshift eliminates all galaxies more than 3500 arcsec from the cluster center. This

is why the velocity dispersion reported in Table 1 is so different depending on the choice of cutoff radius.

3.4. A1749

In A1749, there are 6 galaxies in the velocity range $19000 - 20000 \text{ km s}^{-1}$ which survive the 3σ clipping to provide a non-Gaussian velocity distribution in this cluster, as well as an inflated velocity dispersion. As shown in Table 1, the dispersion of these cluster members is 1048 km s^{-1} , while the more robust value of S_{bi} is 791 km s⁻¹. These galaxies on the high velocity tail stand out quite clearly in Fig 3c, where they appear to form a subcluster to the SE of the center of A1749.

3.5. A1927

The kinematics of A1927 are quite unusual. The histogram of velocities shown in Fig 1f appears normal enough, but the spatial distribution of velocities indicates subclustering. The lower panel of Fig 3f shows that a preponderance of galaxies with velocities below the cluster mean (open and solid squares in the plot) lie to the South and West of the cluster center, while those galaxies with velocities larger than the cluster mean (plotted as open and solid triangles) lie to North and East of the cluster center. This situation is similar to spatial velocity distribution that we found for A2107 (Oegerle & Hill 1992). It is difficult to determine the true cause of this distribution; as discussed in Oegerle & Hill (1992), it could just be a coincidental alignment of subclusters about the cD, or it could indicate rotation of the cluster about the cD.

3.6. A2067 and A2061

A2067 is a member of the Corona Borealis supercluster. Consequently, our redshift survey of A2067 includes the nearby cluster A2061, which is to the SW of A2067. The velocity distribution shown in Figure 1 includes velocities from both clusters, resulting in its bimodal appearance. The velocity of the cD in A2067, indicated by the arrow, is 22005 km s⁻¹, while the velocity of the BCG in A2061 (galaxy # 316 in the tables of Paper III) is 23725 km s⁻¹. The fact that A2067 and A2061 are separate clusters is also easily seen in the Dressler-Shectman diagram shown in the upper panel of Fig 3g.

Given the projected spatial separation on the sky of ~ 30 arcmin for the brightest cluster

members and their 1720 km s⁻¹ difference in radial velocity, it is possible to crudely separate the two clusters by a simple consideration of each galaxy's velocity and position. For each galaxy, we compute a threshold velocity, $v_t = \bar{v} - \delta v | r_1 - r_2 | / 2r_{12}$, where \bar{v} is the average of the A2067 and A2061 BCG velocities, δv is the absolute value of the difference in velocities of the BCGs, r_1 is the distance of the galaxy to the cD in A2067, r_2 is the distance of the galaxy in question is greater than v_t , then that galaxy is assigned to A2061; otherwise it is assigned to A2067. This probabilistic separation technique is not by any means unique, but it is certainly more representative of the distributions of the individual clusters. The velocity histograms for the resulting members assigned to A2067 and A2061 are shown in Figure 2. The results quoted in Table 1 are for A2067 only as determined from our separation. 200 velocities from Small, Sargeant & Hamilton (1997) have been included in this analysis of the clusters A2067 and A2061. Small et al. (1998) discuss the structure and dynamics of the larger supercluster.

Dynamical results for A2061 are not reported in Table 1, since this cluster is not a member of our cD sample, but will be reported here. Based on 126 observed velocities (after separating out those belonging to A2067), the number of probable cluster members surviving the 3σ clipping is 118. We find a mean observed velocity of 23721 ± 67 km s⁻¹, and a biweight location of $C_{bi} = 23699\pm70$ km s⁻¹. The standard velocity dispersion is 673^{+49}_{-40} km s⁻¹, and the biweight scale is 780^{+57}_{-47} km s⁻¹.

3.7. A2079

A2079 is also a member of the Corona Borealis supercluster. The cluster analysis is complicated by several groups of galaxies near 25000 km s⁻¹. These groups of high velocity galaxies are evident in the Dressler-Shectman diagram in Fig 3h. These groups are located ~ 2500 arcsec to the East and NW of the cluster center. These galaxies are not easily rejected by 3σ clipping or by the biweight estimators. Therefore we report velocity and dispersion results in Tables 1, 2 and 3 based on a restricted radius of 2200 arcsec (2.77 h_{75}^{-1} Mpc) around the BCG. The galaxies outside this radius are shown in Figures 1h and 3h. The over-plotted Gaussian in Figure 1h represents the result from all the velocities, and not the dispersion from the restricted radius. After exclusion of these outlying galaxies, the velocity distribution in A2079 passes the I statistic test for Gaussianity, and the Dressler-Shectman test indicates no further evidence for subclustering.

3.8. A2089

A2089 is also part of the Corona Borealis supercluster, however it does not have severe problems with overlapping clusters or groups. Our analysis includes 50 redshifts from Small, Sargeant & Hamilton (1997), although many of them are background galaxies. A spatially distinct group of galaxies lies ~ 1700 arcsec to the West of the A2089 cD galaxy. When these galaxies are included in the cluster, the velocity distribution is non-Gaussian and the Dressler-Shectman test indicates that the subclustering is significant at the 2σ level (i.e. only $\sim 8\%$ of the simulated clusters had $\Delta_{sim} > \Delta_{obs}$). With a radius cutoff of $1.5h_{75}^{-1}$ Mpc, the cluster galaxies have a Gaussian velocity distribution with no subclustering.

3.9. A2199

A2197 is a neighboring cluster to A2199, and has roughly the same redshift. However, the vast majority of the galaxies observed by us are easily identified as belonging to A2199. We have excluded from the A2199 analysis those galaxies which lie North of declination +40.25 degrees, defined as the boundary between A2197 and A2199 by Gregory & Thompson (1984). The cluster passes the I statistic test for having a Gaussian velocity distribution, although the Dressler-Shectman statistic indicates subclustering at a marginally significant ($\sim 2\sigma$) level. Recent X-ray images of A2199 have shown that the hot, X-ray emitting gas, which presumably follows the shape of the gravitational potential, is elongated in shape (Siddiqui, Stewart & Johnstone 1998). In addition, a study of this cluster in the radio and X-ray by Owen & Eilek (1998) indicates that the core of A2199 is complex, and a simple, spherical cooling flow model cannot reproduce the observed data.

3.10. A2666

A2666 is located in the background of the Perseus-Pisces supercluster along with A2634 and A2622. Scodeggio et al. (1995) provide a detailed study of the supercluster environment. Here we concentrate on the A2666 itself. The field includes galaxies at the velocity of A2622 even though that cluster is 3 degrees to the West. This is a very poor cluster (Abell richness class 0), and the galaxies within $1.5h_{75}^{-1}$ Mpc have a very small velocity dispersion (307 kms⁻¹ as reported in Table 1). This dispersion is inflated to 593 km s⁻¹ when considering a larger field of view, presumably due to the inclusion of galaxies affected by the supercluster kinematics.

4. PECULIAR VELOCITIES OF cD GALAXIES

One of the principal goals of this survey is to determine the nature and frequency of peculiar velocities of cD galaxies. We define cD peculiar velocity as $v_p = v_{cD} - v_{cl}$, where v_{cl} is the mean velocity of the cluster, with all velocities cosmologically corrected. Peculiar velocities for all the clusters in the sample are reported in Table 3. We have also tabulated the "robust" peculiar velocity, $v_{pr} = v_{cD} - C_{bi}$, which employs the biweight location instead of the mean cluster velocity. The significance of these peculiar velocities depends on both the uncertainty in the velocity of the cD galaxy, ϵ_{cD} , and the uncertainty in the mean velocity or biweight location, ϵ_{cl} , of the cluster potential well. The uncertainty in the latter quantity is a function of the cluster velocity dispersion and the number of measured galaxies. Table 3 also lists the significances, S, following the nomenclature of Sharples, Ellis & Gray (1988) and Hill $et\ al.\ (1988)$ where $S=|v_p|/\sqrt{\epsilon_{cD}^2+\epsilon_{cl}^2}$, and $\epsilon_{cl}^2=\sigma_{cl}^2/N_{cl}$. The robust significance, S_r , is computed in an analogous manner using v_{pr} and $\epsilon_{cl}^2=S_{bi}^2/N_{bi}$.

Using the robust significance, S_r , and restricting the radius to $1.5h_{75}^{-1}$ Mpc, only 4 of the 25 cD galaxies have a significant $(S_r > 3)$ measured peculiar velocity – A2052, A2107, A2199 and A2670. Detailed dynamical studies of the four clusters with significant peculiar velocities have been reported by Malumuth *et al.* (1992) (A2052), Oegerle & Hill (1992) (A2107), this discussion above (A2199) and Bird (1994) (A2670).

A histogram of the measured peculiar velocities of the 25 cD galaxies is shown in Figure 4. The total range of peculiar velocities is quite small, being confined to a value less than 400 km s⁻¹. We have analyzed the distribution of robust peculiar velocities, v_{pr} , reported in Table 3, by treating them as a psuedo-cluster of galaxies. These 25 peculiar velocities were then analyzed with the same suite of dynamical analysis tools that were used to analyze the individual clusters. The mean absolute deviation of the distribution of peculiar velocities is 168 km s⁻¹. The observed distribution appears rather flat, and is non-Gaussian according to the I statistic test. We find that the distribution of peculiar velocities has a biweight location of 42 ± 33 km s⁻¹ which is consistent with zero net velocity, as one would expect for the radial (projected) distribution of any set of galaxies drawn randomly from a sample of clusters. The biweight scale of the distribution of peculiar velocities is 204 km s⁻¹, but decreases to 164^{+41}_{-34} km s⁻¹ when corrected for the measurement uncertainties reported in Table 3. We interpret this as a significant detection of a velocity dispersion of central cD galaxies around their individual cluster mean velocities.

These results refute the traditional hypothesis that cD galaxies lie exactly at rest in their cluster potential wells assuming that the clusters are virialized. However, the same results confirm that cD galaxies have a substantially lower velocity than the typical galaxies in their clusters. The biweight scale of 164 km s⁻¹ in cD peculiar velocities is much less than

the mean biweight scale, 869 km s⁻¹, for the clusters in this sample.

Peculiar velocities of cD galaxies, and our interpretation of them, must be scrutinized carefully, since there are a number of subtle, and not so subtle effects, which can drastically alter their true value. Futhermore, the root physical cause of a peculiar velocity may not be evident in the kinematical information. Below, we discuss several of these effects.

4.1. Measurement Errors

Whether or not a peculiar velocity is significant depends on the velocity measurement errors for the cD galaxy, and on the uncertainty in the mean velocity of the cluster as influenced by the finite number of galaxies measured and the cluster velocity dispersion. Repeated observations of the cD galaxies in our sample have allowed us to measure their velocities fairly accurately. Typical uncertainties for the cD velocities are $\sim 30 \text{ kms}^{-1}$. Hence, for a given individual cluster, the measurement error is dominated by the uncertainty in the mean velocity of the cluster, which scales as $\sigma_{cl}/\sqrt{N_{cl}}$, typically $\sim 70-100 \text{ km s}^{-1}$. We can then see that, in order to maintain constant measurement errors for a sample of clusters, it is more difficult to measure a statistically significant peculiar velocity in a high dispersion cluster, since the number of cluster member velocities which must be determined goes up as the square of the dispersion. This is illustrated in Figure 5, which shows the absolute value of the robust peculiar velocity plotted against the robust dispersion (biweight scale), S_{bi} , of the cluster. The error bars on the points reflect the uncertainties in the peculiar velocity and the biweight scale respectively. The clusters with larger dispersions have larger uncertainties in C_{bi} , and thus it is more difficult to measure a significant peculiar velocity in those clusters.

4.2. Substructure

Substructure can affect the mean cluster velocity and velocity dispersion, and hence affect the computed peculiar velocity of the cD. What we really desire to know is whether or not the cD galaxy has a peculiar velocity with respect to the bottom of the potential well of the cluster. Substructure in the core of a cluster can obviously result in a peculiar velocity of the central galaxy. Small subclusters at relatively large distances from the cluster core are dynamically unimportant to the motion of the cD galaxy. However, their inclusion can sometimes substantially alter the computed mean cluster velocity. This can then produce a false signal of peculiar velocity of the cD galaxy with respect to the cluster.

If we consider all the measured galaxies within $3.5h_{75}^{-1}$ Mpc of the cDs in our sample,

then the cDs in clusters A1927, A2052, A2079, A2107, A2199, A2634 and A2670 all have an apparently significant peculiar velocity relative to the cluster mean velocity. This should be compared with the result reported above that only four clusters had cDs with peculiar velocities when galaxies within $1.5h_{75}^{-1}$ Mpc were used in the analysis. These four clusters have 68 or more member velocities each within $1.5h_{75}^{-1}$ Mpc, so the different results obtained within these two radii are not principally due to decreased statistical uncertainty. Clearly, the success with which we are able to sort out spatial and velocity outliers from the projected cluster distribution has a large effect on the computed peculiar velocities of cDs.

We note an apparent absence of cDs with large peculiar velocities in the low dispersion clusters (see Figure 5). If cD galaxies form in low mass groups which then merge with more massive clusters, then we might expect to find just as many cD galaxies with peculiar velocities in low mass clusters as in higher mass clusters. Alternately, if cDs form in low velocity dispersion groups and have time to come to rest in that potential well, then we might expect them to have smaller peculiar velocities in that environment, and large peculiar velocities after the merger into the larger cluster. This is very difficult to evaluate because poor groups and clusters do not have enough galaxies in them to give a good measurement of the mean cluster velocity. However, the small number of low mass (low dispersion) clusters in this sample is not adequate to address this issue.

In Figure 6, we have plotted the fraction of simulated clusters containing more apparent substructure than the observed cluster, $f(\Delta_{sim} > \Delta_{obs})$, against the robust significance, S_r . We see that three of the four clusters with $S_r > 3$ show small values of f implying that they have statistically significant substructure as detected by the Dressler-Shectman test. Not all varieties of substructure are necessarily detected by the Dressler-Shectman test, so substructure could account for all the significant peculiar velocities that we observe. See Pinkney et al. (1996) for a summary of the various statistical tests available to study substructure. Alternately, the absence of clusters in the upper right corner of Figure 6 indicates that clusters without substructure do not have cDs with significant peculiar velocities.

Mergers of subclusters and groups into a massive cluster also have the possibility to disturb a cD galaxy from its resting place at the bottom of the potential well. Zabludoff & Zaritsky (1995) present observations of the cluster A754 which they argue is the result of a collision between two subclusters. While this is an extreme example, it serves to illustrate that mergers can disrupt the location and/or velocity of a cD galaxy. Smaller mergers would be expected several times during the lifetime of a cluster. Pinkney et al. (1993) suggest that such a merger could have resulted in the peculiar velocity of the cD galaxy in A2634, although that peculiar velocity is only marginally significant. Bird (1994) also reports evidence for two or more subclusters in A2670 which may be the remnants of the groups which formed

the rich cluster.

4.3. Galaxy Mergers and Interactions with the cD

cD galaxies often contain multiple nuclei, that potentially can exert a gravitational influence on the primary nucleus, either through mergers or by dynamical interactions. Hoessel (1980) finds that 28 - 45% of brightest cluster galaxies (BCGs) contain secondary nuclei within $10h_{75}^{-1}$ kpc of the center of the BCG, which is too high a fraction to be explained by chance superposition. Lauer (1988) has performed a photometric study of the light profiles of 16 multiple nucleus BCGs and found evidence for interactions between the multiple nuclei and the BCG in about half the cases. In many cases, these nuclei are moving through the cluster core too rapidly to merge with the BCG. Lauer (1990) suggests that only 25% of the multiple nuclei systems are currently merging with the BCG.

Consider the effects of a high speed encounter of a galaxy of mass m_g moving through the cluster core with velocity v_g . The impulse approximation will hold for passage within a distance $b = r_{cD}v_g/\sigma_{cD}$ of the cD galaxy, where r_{cD} and $\sigma_{cD} \approx \sqrt{Gm_{cD}/r_{cD}}$ are the radius and velocity dispersion of the cD galaxy, respectively. The perpendicular velocity component of the impulse, which is substantially larger than the parallel component, is given by

$$\delta v = \frac{2m_g b v_g^3}{G(m_{cD} + m_g)^2} \left[1 + \frac{b^2 v_g^4}{G^2(m_{cD} + m_g)^2} \right]^{-1}$$

(Binney & Tremaine 1987). The second term in brackets above is $\gg 1$, so that $\delta v \approx 2Gm_g/bv_g$. If we assume that the perturbing galaxy's mass has been tidally truncated with a value given by $m_g/m_{cD} \approx (\sigma_g/\sigma_{cD})^3$, and $b = r_{cD}v_g/\sigma_{cD}$, we then derive the result $\delta v \approx 2\sigma_g^3/v_g^2$. With values $v_g = 1000~{\rm km\,s^{-1}}$ and $\sigma_g = 200~{\rm km\,s^{-1}}$, the velocity kick imparted to the cD is $\sim 16~{\rm km\,s^{-1}}$. On average, the observed (projected) peculiar velocity would be $\delta v/\sqrt{3} \sim 10~{\rm km\,s^{-1}}$. Even this relatively small velocity kick will decay fairly quickly due to dynamical friction. Lauer (1988) derives the characteristic decay time of this velocity to be $\approx 0.5t_c$, where t_c is the crossing time of the perturbing galaxy. For representative impact parameters and velocities, the decay time is $\sim 10^8$ years. Hence, perturbations in the velocity of the cD nucleus will be damped out fairly quickly, and furthermore, there will only be of order one high speed encounter per crossing time. We conclude that velocity "kicks" due to galaxies passing through the cluster core are very unlikely to explain the peculiar velocities that are observed.

Malumuth (1992) has simulated the evolution of galaxy clusters and the formation of cD galaxies by dynamical friction. He finds that after 10¹⁰ years only a few percent of central

galaxies have projected peculiar velocities larger than 300 km s⁻¹. Looking earlier in the simulations at the epoch where the cDs are born roughly doubles the number with large peculiar velocities, but that number is still well below what we observe. We find that our data are still in agreement with Malumuth's conclusion that cDs formed in virialized clusters would have a distribution of peculiar velocities which is inconsistent with (smaller than) the observed distribution.

We have tried to obtain velocities of extra nuclei of the BCGs if they are comparable in brightness (and hence mass) to the primary nucleus. It was not possible to obtain velocities of all multiple nuclei, and hence we have relied on measurements by other authors who have specifically studied multiple nuclei (Tonry 1984, 1985; Hu et al. 1985; Blakeslee & Tonry 1992).

5. FORMATION SCENARIOS FOR cD GALAXIES

Our question at the beginning of this decade-long dynamical survey of cD clusters of galaxies was whether the number and distribution of cD peculiar velocities would be able to constrain the models of cD formation and growth.

The notion that cD galaxies have formed over a long period of time in the center of a rich cluster of galaxies due to cannibalism or mergers (the post-collapse model) has given way in recent years to the idea that cD galaxies formed long ago prior to cluster collapse and virialization. Merritt (1985) and Lauer (1988) have argued that the large luminosities of cDs cannot be built over a cluster lifetime based on dynamical friction rates. Our observations of substructure seem to support the idea that cD galaxies live in clusters which are dynamically young and not completely virialized.

West (1994) has pointed to the cD "alignment effect" (the fact that cD halos are preferentially elongated in the direction of large scale-structures of galaxies) as evidence that cDs are formed by a process of mergers of clumps of mass which fall anisotropically along preferred axes whose orientations are related to the large-scale density field. In this formation mechanism, cD galaxies are born early in the life of the cluster, as the cluster forms around the cD. Dubinski (1998) has made a detailed cosmological simulation of cluster collapse. He finds that the central galaxy forms through a merger of several massive galaxies in a filament early in the clusters' history. cD galaxies formed in this manner would be expected to lie at the bottom of the potential well, unless late merging of subclusters disrupted the potential well slightly.

Zabludoff & Mulchaey (1998) have argued that cD galaxies form from galaxy-galaxy

collisions in poor groups of galaxies, where merger efficiencies are improved by the low group velocity dispersions. These poor groups, with their central massive galaxies, then merge with other poor groups or fall into existing clusters. This model is attractive in that it explains the existence of cD galaxies in relatively poor clusters, and provides a natural explanation for the cD peculiar velocities that we observe. However, it is not clear how a cD envelope would survive the tidal shear as it falls into a massive cluster. If all cDs formed initially in poor groups of galaxies and then later merged their way into the center of rich clusters, then a larger sample of clusters might be expected to show a few clusters where the cDs had very large peculiar velocities. In this sample of 25 clusters, we do not see any peculiar velocities as large as the cluster velocity dispersion.

6. CONCLUSIONS

We have completed a dynamical study of a complete sample of 25 clusters of galaxies with central cD galaxies. Redshifts for galaxies in three of the clusters were obtained from the literature. Redshifts for the other 22 clusters were taken from our own observations combined with velocities from the literature. The number of cluster member galaxies with observed velocities ranged from 38 to 236 per cluster.

We have reported the detailed dynamical results for the 11 clusters for which we presented data in Paper III. In addition, we have recomputed the dynamical properties for all 25 clusters in the sample using our own data combined with redshifts from the literature. Robust statistical estimators (Beers, Flynn & Gebhardt 1990) of mean cluster velocity and dispersion (biweight location and scale) have been used to carefully assess the significance of our results, which are summarized below.

Of these 25 clusters, four show significant peculiar velocities of the cD galaxies relative to the cluster biweight location (i.e. robust mean velocity) using the criterion that $S_{\tau} > 3$ for galaxies within $1.5h_{75}^{-1}$ Mpc of the cD. Those clusters are A2052, A2107, A2199 and A2670 with peculiar velocities between 250 and 400 km s⁻¹. The distribution of all cD peculiar velocities in our sample has a biweight scale (i.e. robust dispersion) of 164_{-34}^{+41} km s⁻¹, indicating that cD galaxies are not strictly at rest with respect to the potential wells of their parent clusters.

We confirm the existence of peculiar velocities of cD galaxies relative to the mean velocity of their clusters. However, cD peculiar velocities and their dispersion are significantly lower than the velocity dispersions of the cluster galaxies in the survey, making them kinematically distinct from the rest of the cluster population. Therefore, we also confirm the traditional

view that cD galaxies are approximately at rest in their cluster potential well.

Having established the statistical reality of cD peculiar velocities, we have considered the origin of these velocities. Various authors (Hill et al. 1988; Malumuth 1992) have explored galaxy-galaxy interactions and multiple nuclei in the vicinity of the cD as the causes of the peculiar velocities. However, the amplitudes and frequency of the observed peculiar velocities are greater than expected.

Of the 25 clusters surveyed here, 8 of them ($\sim 30\%$) show evidence of subclustering at the 90% confidence level (i.e. $f(\Delta_{sim} - \Delta_{obs}) < 0.1$) when considering galaxies within $1.5h_{75}^{-1}$ Mpc of the cluster center. When the cluster radius is extended to $3.5h_{75}^{-1}$ Mpc 13 clusters ($\sim 50\%$) in the survey show evidence of substructure. This level of subclustering is in good agreement with that reported by other investigations using optical or X-ray surveys (Geller & Beers 1982; Dressler & Shectman 1988; West, Jones & Forman 1995; Solanes, Salvador-Solé & Gonzáles-Casado 1999). From this we conclude that cD clusters are dynamically no different than other present-day clusters of the same richness. Furthermore, since dynamical evolution would be expected to erase substructure within several cluster crossing times, the presence of subclustering indicates that cD clusters are still evolving.

Substructure in these clusters appears to be the cause of the observed cD peculiar velocities. Of the four clusters with significant cD peculiar velocities, three of them have significant subclustering (see Figure 6). As the clusters continue to form, subclusters fall in to the parent cluster thereby modifying the cluster potential well. This process could allow the cD galaxy to remain nearly at rest in its local environment while still having a mild peculiar velocity relative to the cluster as a whole.

Our dynamical data reported above do not lead us to a definite conclusion about the formation mechanism of cD galaxies. However, we now have better observational constraints to place on those models. Whether formed in situ or elsewhere, present-day cD galaxies must be nearly at rest with respect to the cluster potential, but not exactly at rest. The small peculiar velocity of the cD galaxies may be either a residual effect from their formation, or the result of recent interactions and mergers of the cluster as a whole. Future kinematic studies of cD clusters at high redshift may provide the necessary clues to the origin of cD galaxies.

This work was partially supported by NASA through grant NAGW-2988 to W. Oegerle at Johns Hopkins University, and NICMOS GTO grant NAG5-3042 to J. Hill at the University of Arizona. Oegerle would like to acknowledge the hospitalities of Steward Observatory and Kitt Peak National Observatory during visits when much of this paper was written.

We thank John Huchra for supplying us with up-to-date versions of ZCAT (Huchra et al. 1992) for the cross-referencing of velocities in the literature, Tina Bird for providing a digital version of the A2670 velocities published by Sharples, Ellis & Gray (1988), and Oleg Gnedin for helpful comments. This research has also made use of the NASA/IPAC Extragalactic Database (NED) which is operated by the Jet Propulsion Laboratory, California Institute of Technology, under contract with NASA.

REFERENCES

Beers, T. C., Flynn, K. & Gebhardt, K. 1990, AJ, 100, 32

Binney, J. & Tremaine, S. 1987, in "Galactic Dynamics", ed. J.P. Ostriker (Princeton:Princeton University Press)

Bird, C. 1994, ApJ, 422, 480

Blakeslee, J. P. & Tonry, J. L. 1992, AJ, 103, 1457

Danese, L., DeZotti, G. & di Tullio, G. 1980, A&A, 82, 322

Dressler, A. & Shectman, S. 1988, AJ, 95, 985

Dubinski, J. 1998, ApJ, 502, 141

Geller, M. & Beers, T. 1982, PASP, 94, 421

Gregory, S. A. & Thompson, L. A. 1984, ApJ, 286, 422

Hausman, M. A. & Ostriker, J. P. 1978, ApJ, 224, 320

Hill, J. M., Hintzen, P., Oegerle, W. R., Romanishin, W., Lesser, M. P., Eisenhamer, J. D. & Batuski, D. J. 1988, ApJ, 332, L23

Hill, J. M. & Oegerle, W. R. 1993, AJ, 106, 831 (Paper I)

Hill, J. M. & Oegerle, W. R. 1998, AJ, 116, 1529 (Paper III)

Hoessel, J. G. 1980, ApJ, 241, 493

Hoessel, J. G., Gunn, J. E. & Thuan, T. X. 1980, ApJ, 241, 486

Hu, E. M., Cowie, L. L. & Wang, Z. 1985, ApJS, 59, 447

Huchra, J., Geller, M., Clemens, C., Tokarz, S. & Michel, A. 1992, Bull. C.D.S. 41, 31

Jones, C., Mandel, E., Schwarz, J., Forman, W., Murray, S. S. & Harnden, F. R. 1979, ApJ, 234, L21

Krempeć-Krygier, J. & Krygier, B. 1999, Acta Astronomica, 49, 403

Lauer, T. 1988, ApJ, 325, 49

Lauer, T. 1990, in "Dynamics and Interactions of Galaxies", ed. Wielen, R. (Heidelberg:Springer), 406

Malumuth, E. M., Kriss, G. A., Van Dyke Dixon, W., Ferguson, H. C. & Ritchie, C. 1992, AJ, 104, 495

Malumuth, E. M. 1992, ApJ, 386, 420

Matthews, T. A., Morgan, W. W. & Schmidt, M. 1964, ApJ, 140, 35

Merritt, D. 1985, ApJ, 289, 18

Oegerle, W. R. & Hill, J. M. 1992, AJ, 104, 2078

Oegerle, W. R. & Hill, J. M. 1994, AJ, 107, 857 (Paper II)

Oegerle, W. R., Hill, J. M. & Fitchett, M. J. 1995 AJ, 110, 320

Owen, F. N. & Eilek, J. A. 1998, ApJ, 493, 73

Pinkney, J., Rhee, G., Burns, J. O., Hill, J. M., Oegerle, W., Batuski, D. & Hintzen, P. 1993, ApJ, 416, 36

Pinkney, J., Roettiger, K., Burns, J. O. & Bird, C. M. 1996, ApJS, 104, 1

Quintana, H. & Lawrie, D. G. 1982, AJ87, 1

Scodeggio, M., Solanes, J. M., Giovanelli, R. & Haynes, M. P. 1995, ApJ444, 41

Sharples, R. M., Ellis, R. S. & Gray, P. M. 1988, MNRAS, 231, 479

Siddiqui, H., Stewart, G. C. & Johnstone, R. M. 1998, A&A, 334, 71

Small, T. A., Sargeant, W. L. W. and Hamilton, D. 1997, ApJS, 111, 1

Small, T. A., Ma, C-P., Sargeant, W. L. W. and Hamilton, D. 1998, ApJ, 492, 45

Solanes, J. M., Salvador-Solé, E. & Gonzáles-Casado G. 1999, A&A, 343, 733

Struble, M. F. & Rood, H. J. 1987, ApJS, 63, 555

Teague, P., Carter, D. & Gray, P. 1990, ApJS, 72, 715.

Tonry, J. L. 1984, ApJ, 279, 13

Tonry, J. L. 1985, AJ, 90, 2431

West, M. J. 1994, MNRAS, 268, 79

West, M. J., Jones, C. & Forman, W. 1995, ApJ, 451, L5

Yahil, A. & Vidal, N. V. 1977, ApJ, 214, 347.

Zabludoff, A. I. & Mulchaey, J. S. 1998, ApJ, 496, 39

Zabludoff, A. I. & Zaritsky, D. 1995, ApJ, 447, L21

This preprint was prepared with the AAS $\mbox{\sc IMT}_{\mbox{\sc E}}\mbox{\sc X}$ macros v5.0.

- Fig. 1.— Histograms of observed velocities for 11 Abell clusters. The velocity binsize is 200 km s⁻¹. The arrow marks the velocity of the cD. The data for A2067 includes the velocities in the nearby cluster A2061. The dashed line is a Gaussian centered at the biweight location, C_{bi} , and with a $\sigma = (1+z)S_{bi}$, where S_{bi} is the robust biweight scale (dispersion) of the cluster. C_{bi} and S_{bi} are computed from galaxies within $3.5h_{75}^{-1}$ Mpc of the cluster center. The dashed line extends to $\pm 3\sigma$. Plots are shown for clusters (a) A779, (b) A1691, (c) A1749, (d) A1767, (e) A1837, (f) A1927, (g) A2067/A2061, (h) A2079, (i) A2089, (j) A2199 and (k) A2666.
- Fig. 2.— Histograms of observed velocities in A2067 and A2061 after separating the two clusters based on galaxy velocities and positions. The binsize is 200 km s⁻¹. After the cluster separation, the velocities of the brightest cluster galaxies in both A2067 and A2061 are close to their respective mean cluster velocities.
- Fig. 3.— In the upper panel, cluster member galaxies are plotted as open circles, where the diameter of the circle is proportional to ϵ^{δ} , from the Dressler-Shectman test. In the lower panel, the same cluster members are plotted with symbols coded according to where they lie in the cluster velocity distribution. Galaxies with velocities $\bar{v} 3\sigma_r \leq v_{obs} < \bar{v} \sigma_r$ are plotted as open squares, those with $\bar{v} \sigma_r \leq v_{obs} < \bar{v}$ are plotted as filled squares, those with $\bar{v} \leq v_{obs} < \bar{v} + \sigma_r$ as solid triangles, and those with $\bar{v} + \sigma_r \leq v_{obs} \leq \bar{v} + 3\sigma_r$ as open triangles. The cD galaxy is plotted at (x,y) = (0,0), with North at the top of the plot and East to the left. Plots are shown for clusters (a) A779, (b) A1691, (c) A1749, (d) A1767, (e) A1837, (f) A1927, (g) A2067/A2061, (h) A2079, (i) A2089, (j) A2199 and (k) A2666.
- Fig. 4.— Histograms of the distribution of peculiar velocities of the cD galaxies in the 25 clusters using galaxies within $1.5h_{75}^{-1}$ Mpc of the cluster center. The upper histogram uses the peculiar velocity, v_{pr} , relative to the robust biweight location, C_{bi} , of the cluster, while the lower histogram uses the peculiar velocity, v_p , relative to the cluster mean velocity.
- Fig. 5.— The absolute value of the robust peculiar velocity, v_{pr} , is plotted against the biweight scale, S_{bi} , for 25 clusters using galaxies within $1.5h_{75}^{-1}$ Mpc of the cluster center.
- Fig. 6.— The fraction of 1000 simulated clusters (for each real cluster) with $\Delta_{sim} > \Delta_{obs}$ from the Dressler-Shectman test is plotted against the robust significance, S_{τ} of the peculiar velocity for 25 clusters using galaxies within $1.5h_{75}^{-1}$ Mpc of the cluster center.

Table 1. cD cluster velocities and dispersions

	3.7	3.7	3.5		······	~				٠	
Cluster	N_{obs}	N_{cl}	N_{bi}	\bar{v}		C_{bi}		σ		S_{bi}	
A85	172	130	136	16507	± 102	16578	± 100	1097	$^{+76}_{-63}$	1166	$^{+80}_{-67}$
• • •	138	108	113	16486	± 116	16560	± 114	1138	$^{+87}_{-71}$	1211	+92 -75
A193	103	75	78	14566	± 87	14592	± 90	717	$^{+67}_{-53}$	797	+75 -59
• • •	82	72	75	14566	± 88	14590	± 91	708	$^{+68}_{-53}$	787	+76 -59
A399	94	92	92	21527	± 132	21535	± 127	1178	$^{+98}_{-79}$	1220	$^{+102}_{-81}$
• • •	78	76	76	21437	± 148	21420	± 143	1205	$^{+112}_{-88}$	1244	$^{+116}_{-90}$
A401	133	122	122	22084	± 108	22050	± 102	1111	$^{+79}_{-65}$	1124	$^{+80}_{-66}$
	101	94	94	22098	± 130	22057	± 123	1170	+96 -77	1189	+98 79
A779	114	83	83	6742	± 253	6872	± 81	2256	$^{+199}_{-157}$	741	+65 -52
• • •	89	53	64	6812	± 54	6845	± 64	379	$^{+44}_{-33}$	512	$^{+59}_{-44}$
A1651	45	37	39	25322	± 171	25284	± 175	943	$^{+134}_{-94}$	1094	$^{+156}_{-109}$
• • •	35	32	33	25306	± 184	25277	± 182	945	$^{+147}_{-100}$	1048	$^{+163}_{-111}$
A1691	82	70	71	21613	± 96	21637	± 91	751	$^{+73}_{-57}$	765	$^{+74}_{-58}$
• • •	65	59	59	21668	± 107	21686	± 97	751	$^{+81}_{-61}$	748	$^{+80}_{-61}$
A1749	69	51	53	17173	± 158	16800	± 109	1048	$^{+123}_{-91}$	791	+93 -69
• • •	68	51	53	17173	± 158	16800	± 109	1048	$^{+123}_{-91}$	791	+93 -69
A1767	64	59	59	21076	± 119	21125	± 109	842	$^{+91}_{-69}$	838	+90 -68
	59	57	57	21077	± 123	21128	± 113	856	$^{+94}_{-71}$	856	$^{+94}_{-71}$
A1795	115	97	102	18730	±88	18772	± 92	806	$+65 \\ -53$	926	$^{+75}_{-61}$
• • •	105	91	96	18723	± 93	18773	± 99	827	+70 -56	966	$^{+81}_{-65}$
A1809	62	54	55	23721	± 111	23702	± 105	740	+84 -63	777	+88 -66
• • •	52	47	47	23757	± 123	23742	± 113	766	+95 -70	776	+96 -70
A1837	65	32	38	20985	± 123	20941	± 156	636	+99 -68	958	$^{+149}_{-102}$
• • •	46	30	34	20956	± 129	20930	± 139	647	+105 -71	811	+132 -89
A1927	76	48	59	28413	±98	28421	± 106	608	+74 -54	814	$^{+99}_{-73}_{+211}$
• • •	43	36	36	29009	± 424	28556	± 243	2276	+329 -229	1460	-147
A2029	90	85	86	23168	± 168	23120	± 159	1436	$^{+125}_{-99}$	1470	+128 -102
• • •	83	80	81	23150	± 175	23096	± 165	1453	+131 -103	1489	+134 -106
A2052	96	73	77	10640	± 90	10561	±89	736	+70 -55	777	$^{+74}_{-58}$
	71	60	62	10611	±83	10593	±79	596	+64 -49	621	$^{+67}_{-51}$
A2063	95	79	80	10474	±78	10485	±77	660	+60 -48	686	$+63 \\ -49 \\ +74$
	70	63	63	10532	±93	10564	± 90	695	+72 -55	712	$^{+74}_{-57}$
A2067	79	70	78	22142	±74	22111	±73	571	$^{+56}_{-43}_{+69}$	641	+63 -49 +69
• • •	46	44	46	22176	±89	22166	± 79	539	-50	536	-50

Table 1—Continued

Cluster	N_{obs}	N_{cl}	N_{bi}	$ar{v}$		C_{bi}		σ		S_{bi}	
A2079	113	89	89	20681	±219	19821	±92	1922	+163 -130	864	+73 -59
	59	52	56	19794	± 107	19766	± 104	711	$^{+82}_{-61}$	778	$^{+90}_{-67}$
A2089	119	72	75	21924	± 101	22028	± 89	793	+76 -59	770	$^{+74}_{-58}$
	46	36	39	22026	± 94	22042	± 95	515	+75 -52	591	+86 -60
A2107	75	68	68	12336	± 86	12338	± 82	674	+67 -52	675	$^{+67}_{-52}$
	75	68	68	12336	± 86	12338	± 82	674	$^{+67}_{-52}$	675	$^{+67}_{-52}$
A2124	64	63	63	19674	± 116	19664	± 107	847	$^{+88}_{-67}$	851	+88 68
	62	61	61	19689	± 119	19684	± 110	858	$^{+91}_{-69}$	862	$^{+91}_{-69}$
A2199	145	137	139	9039	± 69	9017	± 70	780	$^{+52}_{-44}$	826	$^{+55}_{-46}$
	133	127	127	8986	± 71	8948	± 71	775	$^{+54}_{-45}$	796	+55 -46
A2634	176	125	126	9409	± 82	9378	± 78	878	$^{+62}_{-51}$	878	$^{+62}_{-51}$
• • •	137	114	115	9466	± 84	9424	± 81	865	$^{+64}_{-53}$	864	$^{+64}_{-53}$
A2666	67	49	50	8042	± 89	8131	± 81	593	$^{+71}_{-53}$	574	$^{+69}_{-51}$
	54	34	37	8263	± 56	8236	± 58	307	$^{+47}_{-33}$	353	+53 -37
A2670	285	224	236	22840	± 67	22830	± 67	916	$^{+47}_{-41}$	1035	$^{+53}_{-46}$
	226	191	196	22816	±79	22860	±76	1007	+56 -48	1062	+59 -51

Note. — Column 1 is the cluster name. The first line gives the cluster properties based on known redshifts within $3.5h_{75}^{-1}$ Mpc of the brightest cluster galaxy. The second line represents the same cluster with the radius restricted to 1.5_{75}^{-1} Mpc. Column 2 is the total number of redshifts, N_{obs} , in the sample for that cluster. In some cases, identifiable background clusters have been removed. Column 3 is the number of cluster members, N_{cl} , remaining after 3σ clipping. Column 4 is the number of redshifts, N_{bi} , used in the biweight calculations. These are required to be within 6000 km s⁻¹ of the brightest cluster galaxy. Column 5 is the observed mean cluster velocity, $\bar{v} = cz$, in km s⁻¹ after 3σ clipping. Column 6 is the estimated error in the mean cluster velocity in km s⁻¹. Column 7 is the biweight estimate of the observed location, C_{bi} , in km s⁻¹. Column 8 is the estimated error in the location in km s⁻¹. Column 9 is the velocity dispersion, σ , in km s⁻¹ corrected for measurement error after 3σ clipping of galaxy membership. Column 10 is the estimated error in the velocity dispersion in km s⁻¹. Column 11 is the biweight estimate of the scale, S_{bi} , in km s⁻¹ corrected for measurement error and cosmological expansion. Column 12 is the estimated error in S_{bi} in km s⁻¹.

Table 2. Normality and subclustering statistics

			··		
Cluster	I	I_{90}	Δ_{obs}	$f(\Delta_{sim} > \Delta_{obs})$	Notes
A85	0.89	1.04	166	0.039	Gaussian
	0.88	1.05	137	0.062	Gaussian
A193	0.82	1.07	70	0.576	Gaussian
• • •	0.82	1.07	72	0.413	Gaussian
A399	0.93	1.06	85	0.549	Gaussian
	0.94	1.07	67	0.623	Gaussian
A401	0.99	1.04	134	0.255	Gaussian
	0.97	1.05	97	0.406	Gaussian
A779	9.29	1.06	181	0.000	non-Gaussian
	0.56	1.09	42	0.864	Gaussian
A1651	0.75	1.12	21	0.967	Gaussian
	0.84	1.14	20	0.862	Gaussian
A1691	0.96	1.07	68	0.619	Gaussian
	1.00	1.08	52	0.776	Gaussian
A1749	1.79	1.09	81	0.011	non-Gaussian
	1.79	1.09	81	0.011	non-Gaussian
A1767	1.07	1.08	50	0.802	Gaussian
	1.06	1.08	46	0.868	Gaussian
A1795	0.76	1.05	148	0.001	Gaussian
	0.74	1.06	136	0.000	Gaussian
A1809	0.91	1.09	57	0.282	Gaussian
	0.99	1.10	50	0.219	Gaussian
A1837	0.44	1.14	28	0.419	Gaussian
	0.65	1.15	24	0.540	Gaussian
A1927	0.55	1.10	75	0.005	Gaussian
	2.45	1.13	55	0.040	non-Gaussian
A2029	0.95	1.06	99	0.164	Gaussian
	0.94	1.06	95	0.135	Gaussian
A2052	0.92	1.07	74	0.594	Gaussian
	0.94	1.08	58	0.486	Gaussian
A2063	0.93	1.06	71	0.679	Gaussian
	0.96	1.08	54	0.721	Gaussian
A2067	0.80	1.07	94	0.057	Gaussian
	1.03	1.11	52	0.197	Gaussian

Table 2—Continued

Cluster	I	I_{90}	Δ_{obs}	$f(\Delta_{sim} > \Delta_{obs})$	Notes
A2079	5.44	1.06	181	0.000	non-Gaussian
	0.83	1.09	34	0.974	Gaussian
A2089	1.07	1.07	94	0.084	non-Gaussian
	0.75	1.13	25	0.904	Gaussian
A2107	1.00	1.07	111	0.000	Gaussian
	1.00	1.07	111	0.000	Gaussian
A2124	0.99	1.08	67	0.318	Gaussian
	0.99	1.08	64	0.306	Gaussian
A2199	0.90	1.04	176	0.020	Gaussian
• • •	0.95	1.04	151	0.075	Gaussian
A2634	1.01	1.04	165	0.044	Gaussian
	1.02	1.05	150	0.048	Gaussian
A2666	1.07	1.10	71	0.030	Gaussian
	0.78	1.13	45	0.057	Gaussian
A2670	0.78	1.02	308	0.004	Gaussian
	0.90	1.03	261	0.002	Gaussian

Note. — Column 1 is the cluster name. The first line gives the cluster properties based on known redshifts within $3.5h_{75}^{-1}$ Mpc of the brightest cluster galaxy. The second line represents the same cluster with the radius restricted to $1.5h_{75}^{-1}$ Mpc. Column 2 is the I statistic. Column 3 is the I_{90} threshold for the I statistic to indicate a non-Gaussian distribution. Column 4 is the observed Dressler-Shectman Δ statistic. Column 5 is the fraction, f, of shuffled clusters which have Dressler-Shectman Δ greater than the observed cluster.

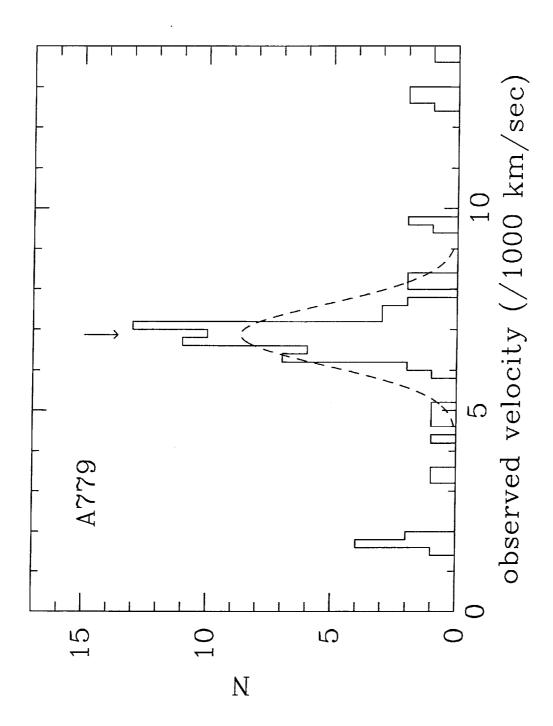
Table 3. cD peculiar velocities

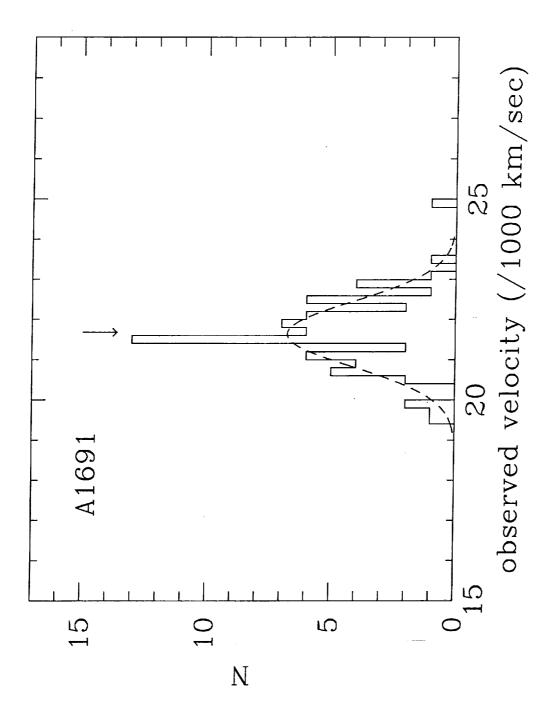
Cluster	v_p		v_{pr}		S	S_r
A85	131	±100	62	±103	1.31	0.60
	151	± 112	79	± 117	1.34	0.67
A193	-93	± 102	-119	± 109	0.91	1.09
	-93	± 102	-117	± 109	0.91	1.07
A399	-134	± 126	-143	± 131	1.06	1.09
• • •	-51	± 141	-36	± 144	0.36	0.25
A401	179	± 114	209	± 115	1.57	1.81
	166	± 131	203	± 134	1.26	1.51
A779	132	± 249	-3	± 75	0.53	0.04
• • •	55	± 55	23	± 67	1.00	0.34
A1651	219	± 167	252	± 186	1.31	1.35
• • •	234	± 178	258	± 192	1.31	1.34
A1691	61	± 91	39	± 92	0.67	0.42
• • •	10	± 90	-7	± 87	0.11	0.08
A1749	-332	± 147	16	± 106	2.25	0.15
• • •	-332	± 147	16	± 106	2.25	0.15
A1767	214	± 114	167	± 114	1.87	1.46
• • •	213	± 118	164	± 117	1.80	1.39
A1795	228	± 83	188	± 93	2.73	2.01
• • •	235	±88	187	± 100	2.66	1.87
A1809	-80	± 100	-63	± 105	0.80	0.60
	-113	± 111	-100	± 112	1.01	0.89
A1837	-233	± 113	-194	± 156	2.05	1.24
• • •	-206	± 119	-182	± 140	1.72	1.30
A1927	436	± 89	429	± 107	4.87	3.99
• • •	-93	± 372	305	± 244	0.25	1.25
A2029	217	± 163	258	± 165	1.33	1.56
• • •	234		280	± 171	1.38	1.63
A2052	-296	± 90	-221	± 92	3.28	2.39
• • •	-269	± 81	-251	± 83	3.30	3.02
A2063	-147	± 78	-158	± 80	1.87	1.96
• • •	-203	± 91		± 93	2.23	2.51
A2067		± 73		±77	1.70	1.25
•••	-157	± 86	-148	± 84	1.82	1.76

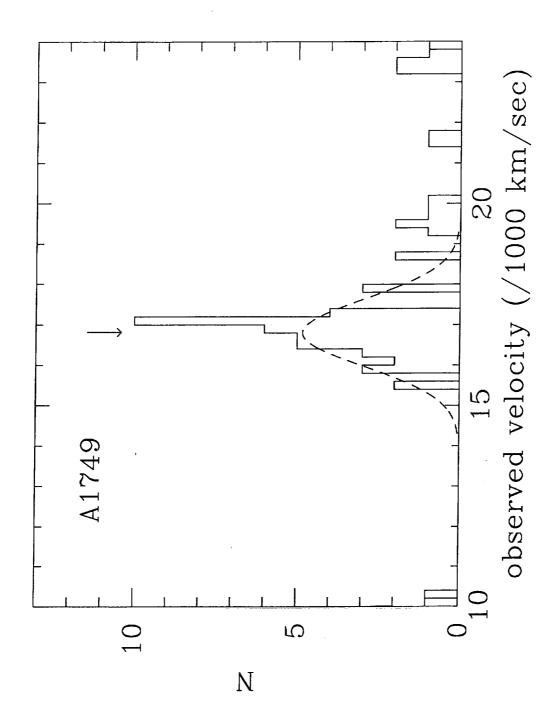
Table 3—Continued

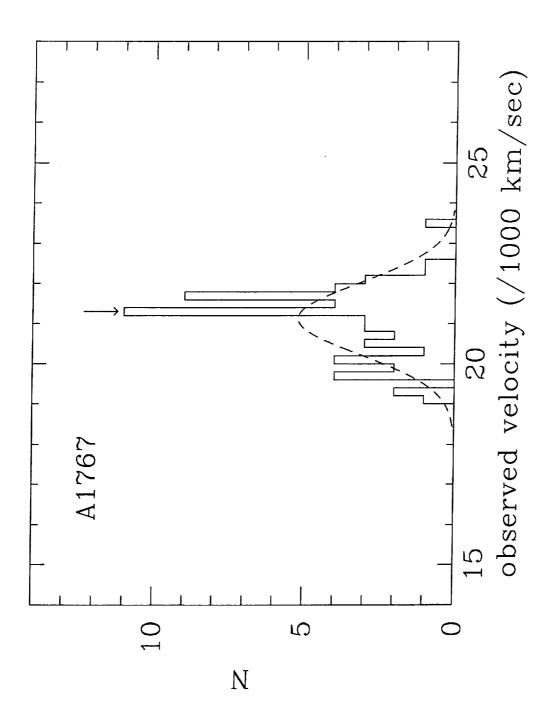
Cluster	v_p		v_{pr}		S	S_r
A2079	-1024	±204	-228	±93	5.01	2.45
	-202	± 100	-177	± 105	2.02	1.68
A2089	142	± 95	44	± 89	1.49	0.49
	47	± 87	32	± 96	0.54	0.33
A2107	270	± 86	266	± 86	3.11	3.07
	270	±86	266	± 86	3.11	3.07
A2124	129	± 111	130	± 126	1.16	1.03
	115	± 113	104	± 130	1.01	0.80
A2199	258	± 69	279	± 72	3.71	3.83
	310	± 71	346	± 73	4.33	4.71
A2634	-245	±96	-216	± 96	2.53	2.24
	-300	± 98	-260	± 98	3.04	2.64
A2666	141	± 87	53	± 84	1.62	0.63
• • •	-74	± 55	-48	± 60	1.33	0.80
A2670	410	± 111	418	± 115	3.67	3.63
	433	±118	390	±120	3.66	3.24

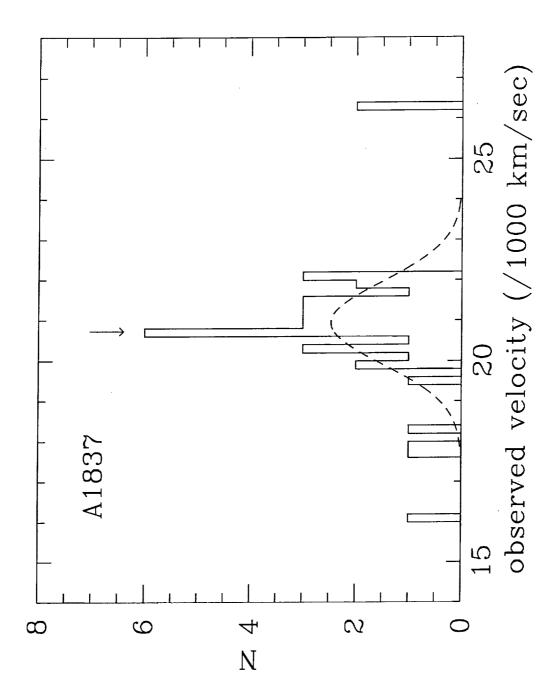
Note. — Column 1 is the cluster name. first line gives the cluster properties based on known redshifts within $3.5h_{75}^{-1}$ Mpc of the brightest cluster galaxy. The second line represents the same cluster with the radius restricted to $1.5h_{75}^{-1}$ Mpc. Column 2 is the cD peculiar velocity, v_p , in km s⁻¹ with respect to the mean cluster velocity with cosmological correction. Column 3 is the error in peculiar velocity in km s^{-1} with respect to the mean cluster velocity. Column 4 is the cD peculiar velocity, v_{pr} , in km s⁻¹ with respect to the biweight location with cosmological correction. Column 5 is the error in peculiar velocity in km s⁻¹ with respect to the bi-weight location. Column 6 is the significance, S, of the peculiar velocity with respect to the mean cluster velocity. Column 7 is the significance, S_r , of the peculiar velocity with respect to the bi-weight location.

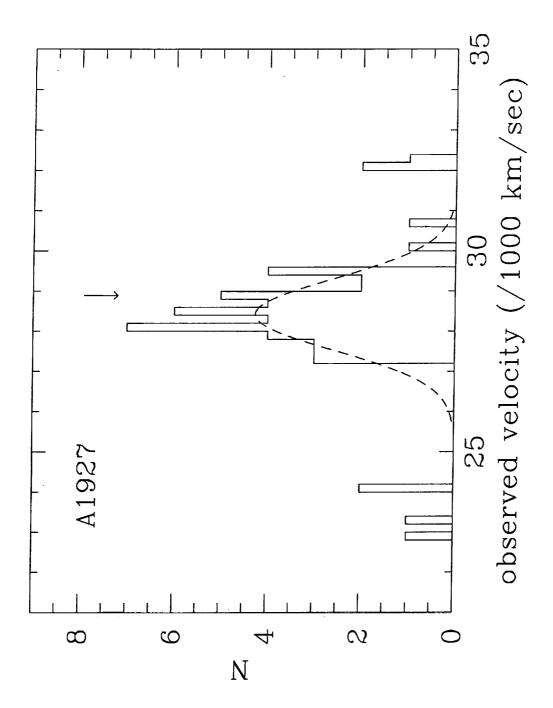


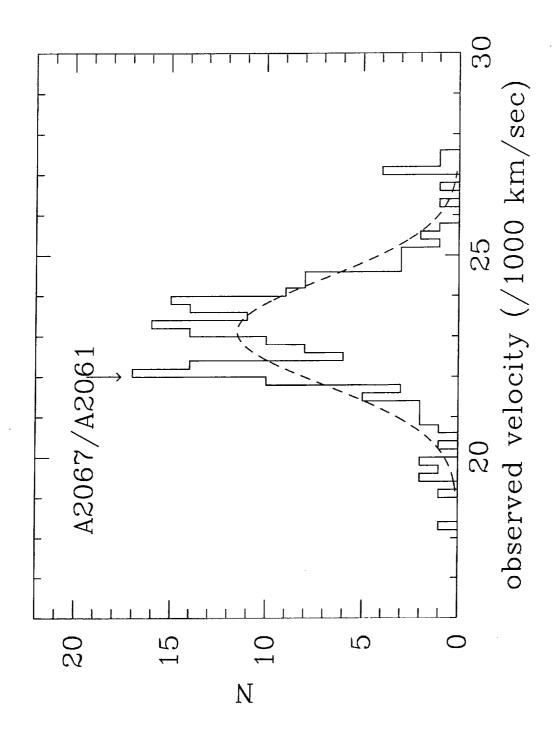


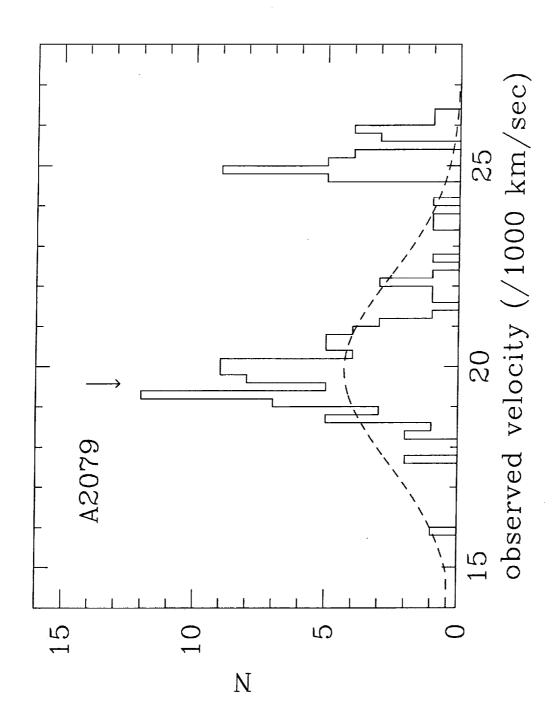


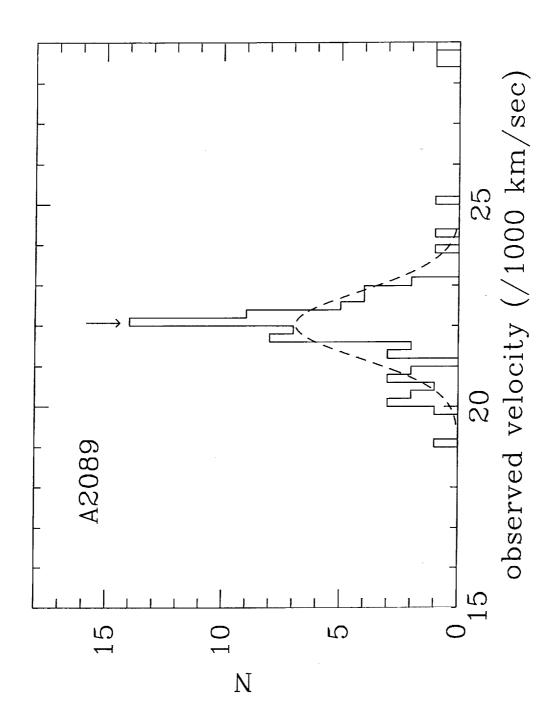


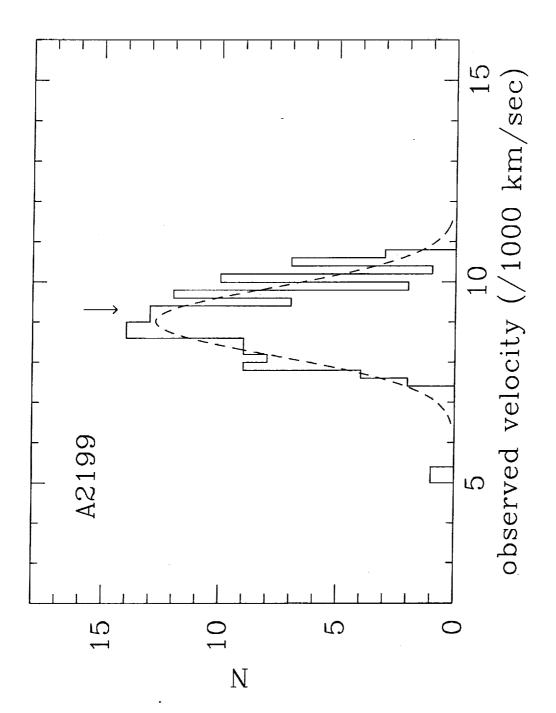


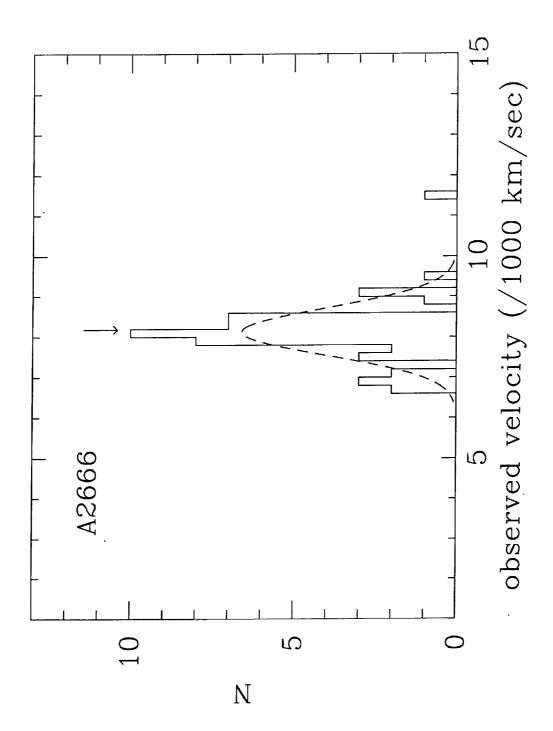


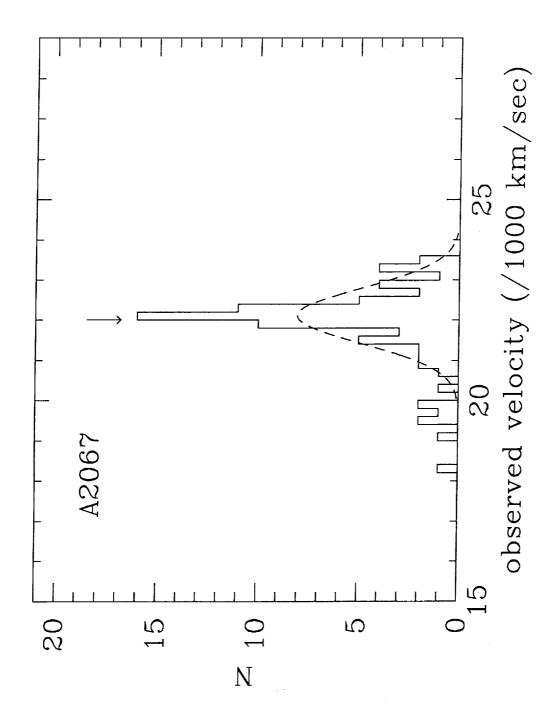


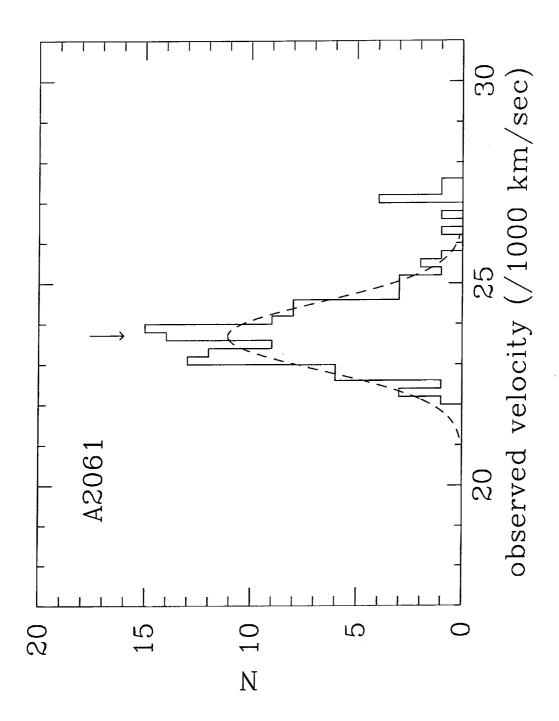


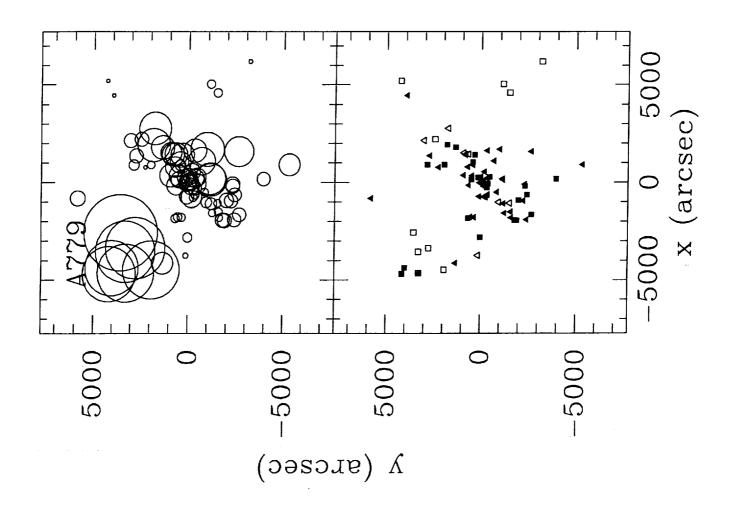


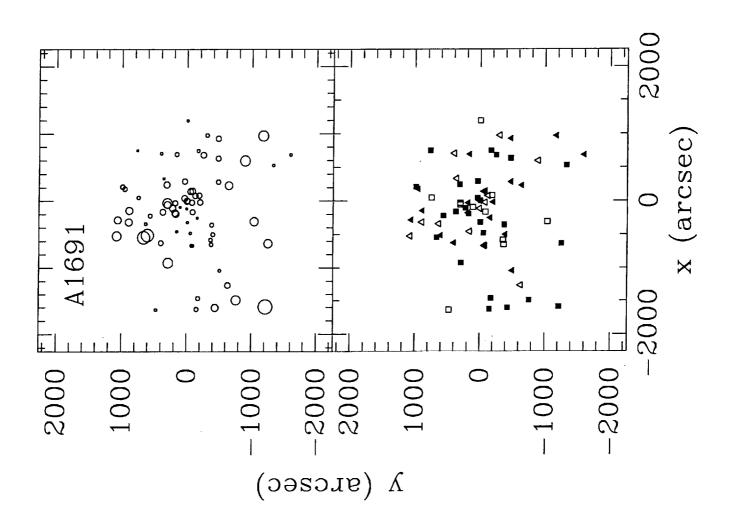


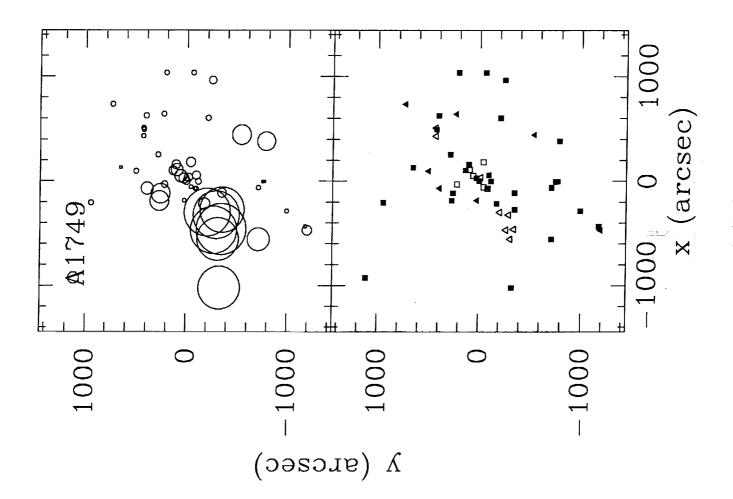


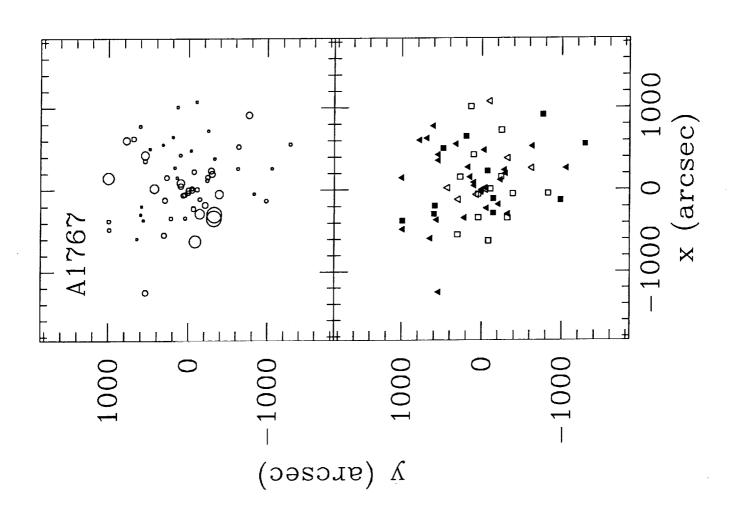


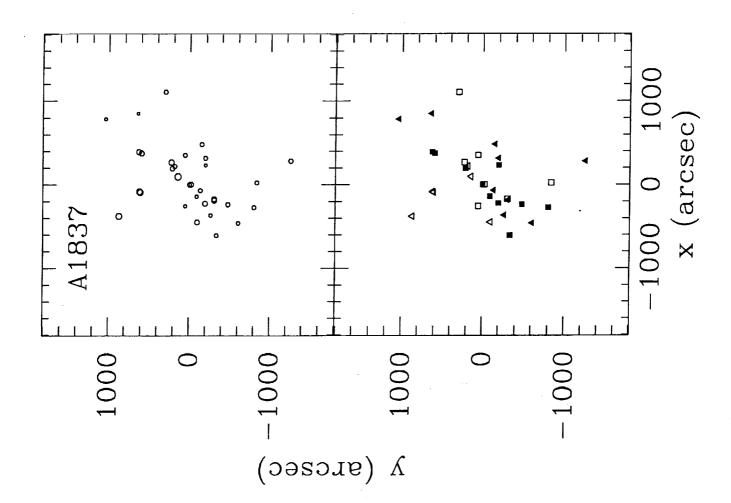


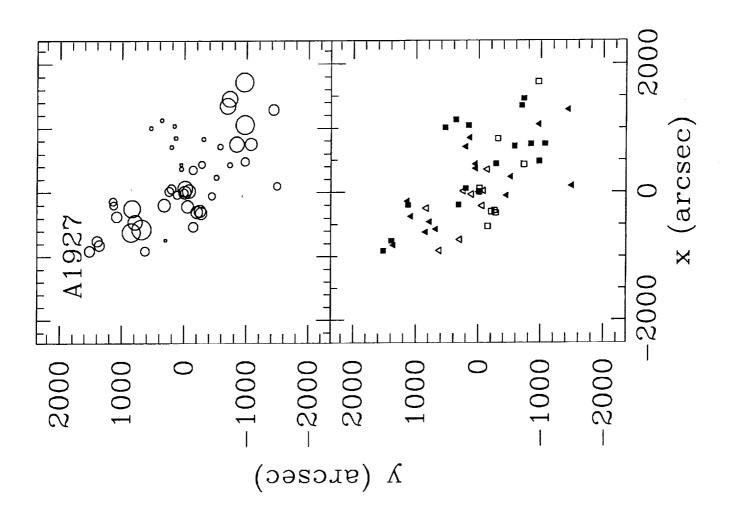


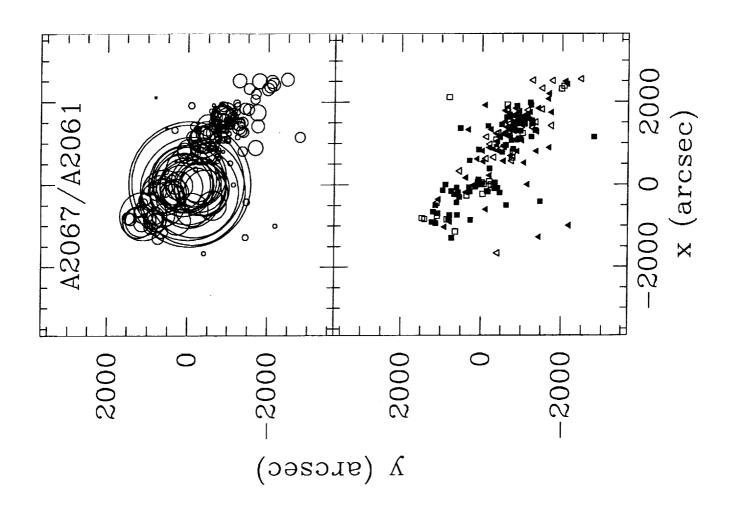


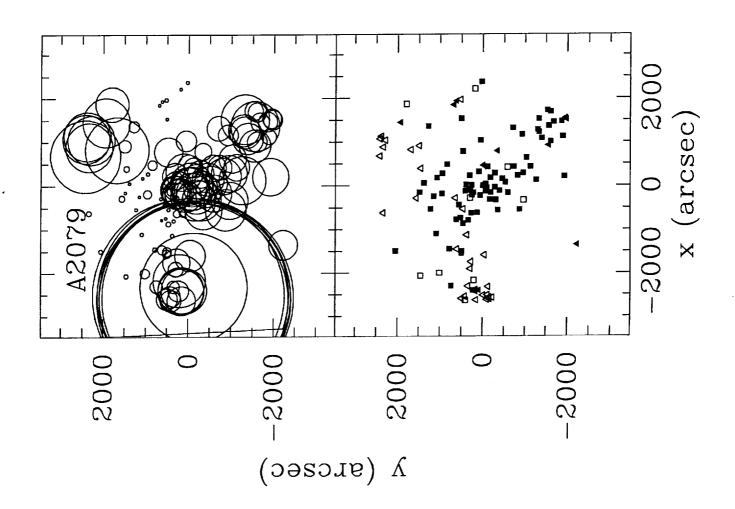


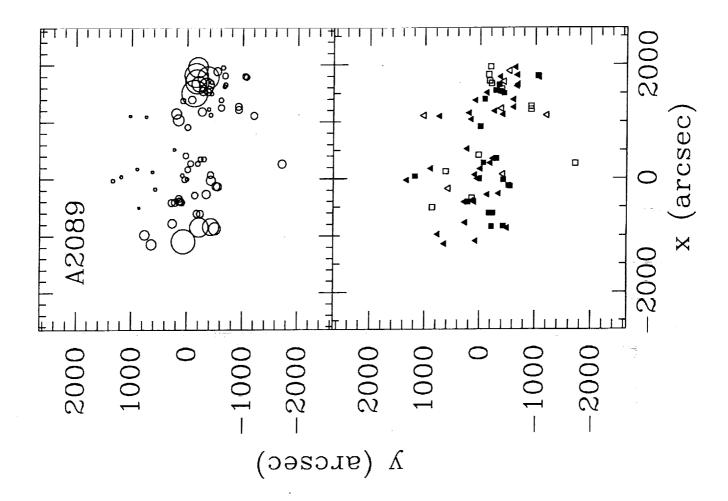


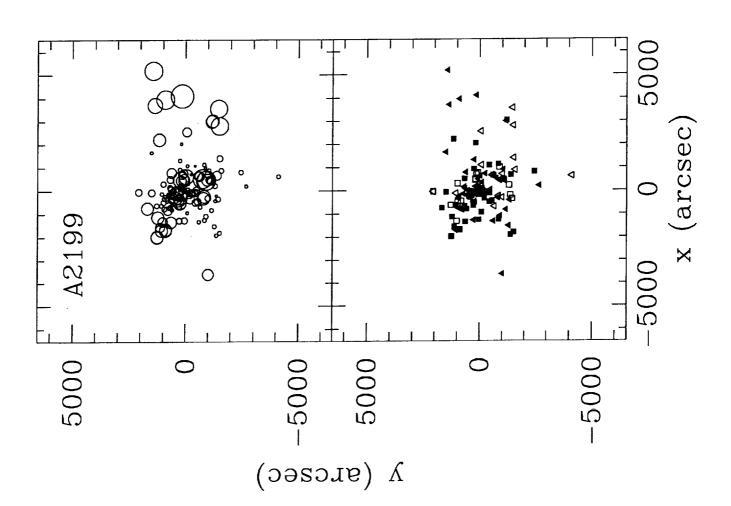


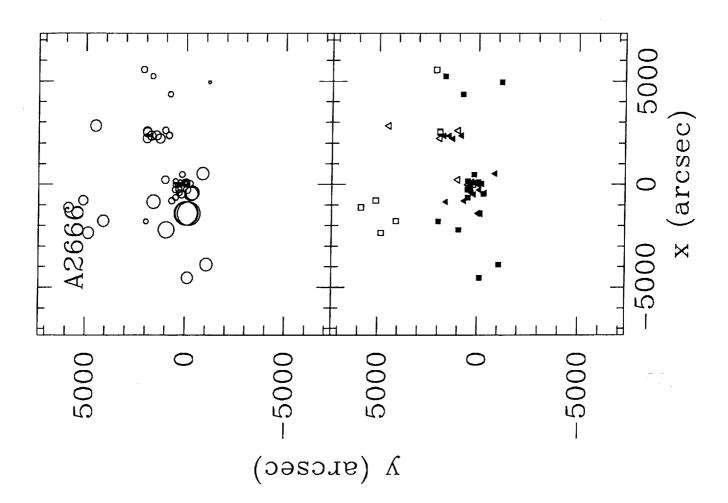


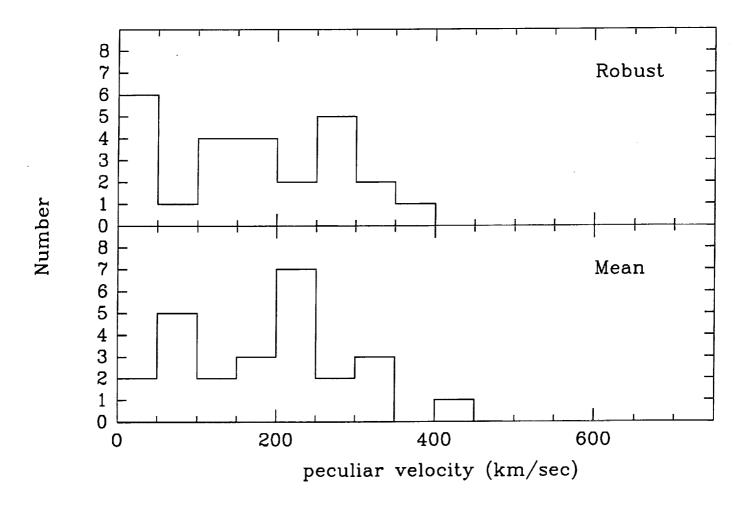


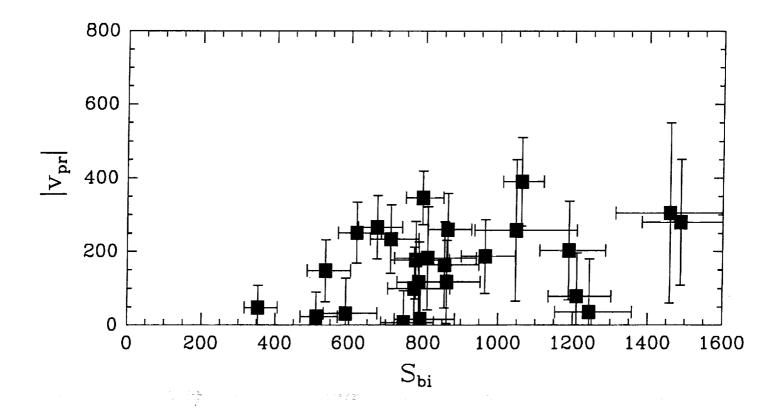


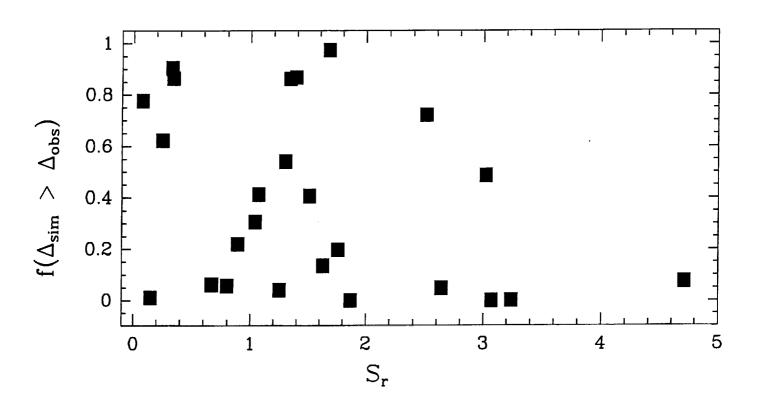












		-	-
·			
	Ē	•••	